ELSEVIER

Journal of Molecular Catalysis A: Chemical 138 (1999) 155–176

JOURNAL OF MOLECULAR CATALYSIS A: CHEMICAL

Hydroformylation of ethene with triphenylphosphine modified rhodium catalyst: kinetic and mechanistic studies

G. Kiss [a,*], E.J. Mozeleski [b], K.C. Nadler [c], E. VanDriessche [c], C. DeRoover [c]

[a] *Corporate Research Laboratories, Exxon Research and Engineering, Annandale, NJ 08801, USA*
[b] *Exxon Chemical, Annandale, NJ 08801, USA*
[c] *Exxon Chemical International, B-1831 Machelen, Hermeslaan 2, Belgium*

Received 9 March 1998; accepted 29 April 1998

Abstract

The kinetics of ethene hydroformylation with triphenylphosphine modified rhodium catalyst has been investigated. The reaction is first order in rhodium. The kinetic order for ethene is also one for most of the reaction conditions investigated, however, the combination of low phosphine and high olefin concentration leads to a saturation in ethene. The kinetic effects of CO and triphenylphosphine are also a function of their concentrations: both inhibit the reaction above a threshold value, while below the threshold a positive kinetic response can be observed. Hydrogen concentration has little effect on the rate of hydroformylation. The olefin hydrogenation selectivity is generally low and can be described as a linear function of the H_2/CO partial pressure ratio. Hydrogenation of the product propionaldehyde cannot be detected by GC. Based on a refined Wilkinson mechanism [C.A. Tolman, J.W. Faller, Mechanistic studies of catalytic reactions using spectroscopic and kinetic techniques, in: L.H. Pignolet (Ed.), Homogeneous Catalysis with Metal Phosphine Complexes, Plenum Press, New York, 1983.], a kinetic model has been developed which fits all experimental observations and can be used to predict reaction rates and selectivities over a wide range of reaction conditions.

Keywords: Hydroformylation; Oxo reaction; Phosphine modified rhodium catalyst; Ethene; Kinetics; Mechanism

1. Introduction

Worldwide hydroformylation (or oxo) capacity in 1993 exceeded 6 million tons/year [2]. Approximately 60% of that capacity is based on the low pressure oxo process (LPO) using phosphine-modified rhodium carbonyls as catalysts. LPO is used to convert light olefins (mainly C_2 and C_3), CO, and H_2 to C_3 and C_4 aldehydes (Eq. (1)). Oxo aldehydes are mainly converted to $C_{n\geq 8}$ alcohols and used in the manufacture of polyvinyl chloride (PVC) plasticizers and detergents.

$$R{-}CH{=}CH_2 + CO + H_2 \rightarrow R{-}CH_2{-}CH_2{-}CHO + R{-}CH(CHO){-}CH_3 \quad R = H \text{ or } CH_3 \qquad (1)$$

The most widely used ligand in LPO is triphenylphosphine (PPh_3). The pioneering work of Evans et al. [3,4], Yagupsky et al. [5] and Brown and Wilkinson [6] has established that (I) in the

* Corresponding author. Fax: +1-908-730-3198; e-mail: gkiss@erenj.com

1381-1169/99/$ - see front matter
PII: S1381-1169(98)00166-6

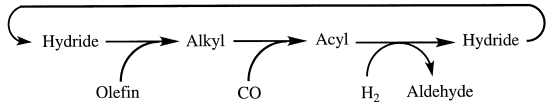

Scheme 1. The main steps of the Heck–Breslow hydroformylation mechanism.

Rh/PPh_3-catalyzed hydroformylation the stable $HRh(CO)(PPh_3)_3$ monocarbonyl hydride complex is a direct catalyst precursor, (II) the major Rh-component present under reaction conditions is the dicarbonyl hydride $HRh(CO)_2(PPh_3)_2$, and (III) the main steps in the catalytic cycle follow the Heck–Breslow mechanism [7–10] developed for the Co-catalyzed oxo reaction (Scheme 1). In order to explain the effect of PPh_3 concentration on product selectivities, Wilkinson proposed two different paths: a dissociative one and an associative one. The former is initiated by the dissociation of CO from the dicarbonyl hydride, and the catalytic cycle follows the 16/18-electron path. The latter is initiated by the association of the olefin with the hydride leading directly to an 18-electron alkyl intermediate via a 20-electron transition state. Later spectroscopic studies [11–25] further refined the details of the mechanism and today it is widely accepted [1,2] that the likely kinetic path is the one which involves 16- and 18-electron species only, i.e., the dissociative mechanism.

While the main features of the mechanism have been well established by identifying spectroscopically observable intermediates, the kinetics of the process have not been thoroughly studied [2]. Although there are some kinetic studies [26–32] which address the effect of several process variables with the goal of developing a kinetic model, only one of them [26] offers an analysis correlating propylene hydroformylation kinetic data with a reaction mechanism. Other publications either offer empirical models [27–32] or focus on a limited number of variables and address only certain aspects (mostly phosphine effect) of the reaction [33–43]. This paper reports the results of a parametric study of the hydroformylation of ethene with triphenylphosphine-modified Rh catalyst. A kinetic model has been developed by correlating the kinetic data with a refined Wilkinson mechanism [1].

2. Experimental

2.1. Materials

Solvents (anhydrous toluene, tetraetheneglycol dimethyl ether, dioctyl phthalate), methylcyclohexane as GC internal standard, all from Aldrich; 2,2,4-trimethyl-1,3-pentanediol monoisobutyrate (or Texanol) from Eastman or ACROS, and isoamyl butyrate from ACROS were thoroughly deaerated but otherwise were used as received. All gases (1:1 H_2/CO, methane, and ethene from MG Industries or Air Liquide), triphenylphosphine (from Aldrich), and $Rh(acac)(CO)_2$ (from Strem or Aldrich) were used as received. All organic compounds were checked for purity by GC (Perkin Elmer Autosystem or Hewlett-Packard 5890, Hewlett-Packard Pona column).

For the kinetic measurements Rh stock solutions were prepared by using the appropriate solvent. The stock solution was made by weighing (0.1 mg accuracy) the solvent, $Rh(acac)(CO)_2$ (acac = acetylacetonato), and PPh_3 (P/Rh ratio of ca. 10) into a bottle. A vigorous evolution of CO suggested the formation of the $Rh(acac)(CO)(PPh_3)$ complex. Catalyst solutions for the hydroformylation of ethene with the desired composition were prepared by weighing the Rh stock solution, additional phosphine, and solvent.

2.2. Apparatus

The batch kinetic experiments were performed in 300 or 500 ml autoclaves (Autoclave Engineers) equipped with speed-controlled mechanical stirrers. The configuration of all units were identical. The reactors were connected to their gas feed vessels (PVT tanks) through a high precision pressure-regulator valve. All volumes in the system were measured by gas volumetric methods. The reactors and feed vessels were equipped with certified Omega digital thermocouples and pressure gauges. The temperature of the reactors was maintained within ± 1°C.

The continuous-flow (continuous stirred tank reactor or CSTR) kinetic experiments were carried out in 500 ml autoclaves (Autoclave Engineers). The reactors were equipped as in the batch units. The gas feed components were fed individually via Brooks mass-flow controllers which were calibrated in-house. All units were equipped with on-line gas chromatographs (MTI or Hewlett-Packard) which sampled both the feed and the effluent. The constant unit pressure was maintained with a back-pressure regulator. The effluent flow was measured with wet-test meters (American meter or Ritter).

The absence of mass transfer limits was verified by variable stirrer-speed experiments. Mass transfer rates for CO, H_2, and C_2H_4 in tetraglyme at different stirrer speeds were also measured using literature methods [44]. The Rh charge at each condition was adjusted to ensure that the liquid phase concentration of the reactants would be above the 95% level of the gas–liquid equilibrium values. Rate and selectivity values obtained in two different reactors at the same condition were statistically indistinguishable. Reproducibility was checked by carrying out at least two runs at each condition.

2.3. Batch kinetic experiments

In a typical experiment, carried out in the 300 ml autoclave, 65 ml of catalyst solution was prepared in a vacuum atmospheres glove-box from the $Rh(acac)(CO)(PPh_3)$ stock solution, PPh_3, and the solvent. The solution was charged into the reactor under nitrogen. The reactor then was flushed and pressurized with syngas (a 1:1 mixture of H_2 and CO) to ca. 500 kPa. Approximately 15 mmol of ethene was also charged into a 75 ml injection bomb which then was mounted into the syngas feed-line of the reactor. The catalyst was preformed in syngas (approximately 500 kPa) at the reaction temperature. NMR and IR experiments were carried out under identical conditions to verify the formation of the equilibrium mixture of rhodium hydrides with a general formula of $HRh(CO)_x(PPh_3)_{4-x}$ ($x = 1$ and 2).

The reaction was initiated by injecting ethene into the reactor and bringing the pressure up to 1000 kPa with syngas. Blank experiments were carried out to test the efficiency of the injection method. In these blank experiments the temperature and pressure in the PVT tank and the reactor equilibrated within 2 min or less. The pressure in the reactor was maintained constant by making up the consumed syngas from the PVT tank. The conversion was followed by recording the pressure drop in the PVT tank. The reaction was stopped by rapid cooling of the reactor typically after 80–95% olefin conversion.

After cooling the reaction mixture, a gas sample was taken into a 50 ml stainless steel bomb. The liquid product was removed under nitrogen. Aliquot samples of the product were prepared under nitrogen for GC analysis by adding known amounts of methyl cyclohexane as a GC internal standard. Mass balances were established for all organic components and were typically $100 \pm 5\%$, except for PPh_3 for which the mass balances were typically $100 \pm 20\%$. The conversions and product selectivities were determined from the mass balance for ethene based on GC analysis of the final liquid and

gas phase, liquid product weight, and gas volume. The later was determined at each reaction temperature from blank experiments.

The rate of reaction was calculated by assuming that the gas consumption, and thus the pressure drop in the PVT tank, is a linear function of conversion. This assumption is valid as long as the pressure of the reactor is constant. The initial pressure of the PVT tank was obtained by extrapolating to time zero on a pressure vs. reaction time plot. The turnover frequency (TOF) used in the kinetic analysis was defined as the rate of olefin conversion by 1 mol of rhodium and expressed as moles ethene converted to aldehydes per mole of Rh per second:

$$\mathrm{TOF} = -\left\{\left(\frac{\mathrm{d}n_{\mathrm{olefin}}}{\mathrm{d}t}\right)\right\}\frac{1}{n_{\mathrm{Rh}}} \tag{2}$$

The rate of olefin conversion was calculated from the PVT pressure vs. time data by approximating the differential $(\mathrm{d}n_{\mathrm{olefin}}/\mathrm{d}t)_t$ with the finite difference $(\Delta n_{\mathrm{olefin}}/\Delta t)_t$ and utilizing the fact that for the consumed olefin $\Delta n_{\mathrm{olefin}} = \text{constant}\ \Delta p_{\mathrm{PVT}}$:

$$(\mathrm{d}n_{\mathrm{olefin}}/\mathrm{d}t)_{t_i} \cong (\Delta n_{\mathrm{olefin}}/\Delta t)_{t_i} = \text{constant}(\Delta p_{\mathrm{PVT}}/\Delta t)_{t_i} \tag{3}$$

where

$$\text{constant} = (\text{total mole of aldehyde product})/(\text{total PVT pressure drop}) \tag{4}$$

For a reaction which is first order in both the catalyst (Rh) and the substrate (olefin), the reaction rate can be expressed as follows:

$$-\mathrm{d}n_{\mathrm{olefin}}/\mathrm{d}t = k[\mathrm{Rh}][\mathrm{olefin}]V_{\mathrm{liq.}} = kn_{\mathrm{Rh}}[\mathrm{olefin}] \tag{5}$$

where $V_{\mathrm{liq.}}$ = liquid volume, and k = reaction rate constant. Then from Eqs. (5) and (2):

$$\mathrm{TOF} = k[\mathrm{olefin}] = kp_{\mathrm{olefin}}/H_{\mathrm{olefin}} \tag{6}$$

where p_{olefin} and H_{olefin} are the partial pressure and the Henry's constant of the olefin, respectively. From Eq. (6) the rate constant, k, can be obtained by using the initial turnover frequency if the initial partial pressure and the Henry's constant of ethene are known. In the text this data analysis will be referred to as 'differential method'.

Another way of analyzing the raw kinetic data is based on the analytical solution of the differential mass balance for the olefin (integral method). For a reaction which is first order in Rh and olefin:

$$-\left(\frac{\mathrm{d}n_{\mathrm{olefin}}}{\mathrm{d}t}\right) = -\left(\frac{V_{\mathrm{gas}}}{RT} + \frac{V_{\mathrm{liq.}}}{H_{\mathrm{olefin}}}\right)\left(\frac{\mathrm{d}p_{\mathrm{olefin}}}{\mathrm{d}t}\right) = k[\mathrm{Rh}]\frac{p_{\mathrm{olefin}}}{H_{\mathrm{olefin}}}V_{\mathrm{liq.}} \tag{7}$$

where V_{gas} = free gas volume in the reactor, R = universal gas constant, T = temperature, other annotations as in Eqs. (2)–(6). From Eq. (7):

$$F\ln\left\{\frac{p_{\mathrm{olefin}}(t)}{p_{\mathrm{olefin}}(t=0)}\right\} = -k[\mathrm{Rh}]t \tag{8}$$

where

$$F = \frac{V_{\mathrm{gas}}H_{\mathrm{olefin}}}{RTV_{\mathrm{liq.}}} + 1$$

Since

$$\frac{p_{\text{olefin}}(t)}{p_{\text{olefin}}(t=0)} = 1 - \text{conversion}(t) \tag{9}$$

$$\ln\{1 - \text{conversion}(t)\} = -(k[\text{Rh}]/F)t = \text{constant}\ t \tag{10}$$

The $\ln\{1 - \text{conversion}(t)\}$ vs. time plot therefore is linear if the reaction is first order in olefin. The rate constant can be calculated from its slope if the free gas and liquid volumes, and the partial pressure and Henry's constant for ethene at the reaction temperature are known.

2.4. CSTR kinetic experiments

The continuous-flow hydroformylation of ethene was carried out in 500 ml Autoclave Engineers' zipperclaves. The catalyst solution was prepared and charged into the reactor as described earlier for the batch experiments. The gaseous feed components, H_2, CO, C_2H_4, and CH_4 (used as GC internal standard and inert diluent), were individually fed via Brooks mass-flow controllers.

Mass balances for each component were obtained independently of each other and typically were $100 \pm 10\%$ for CO and H_2, and $100 \pm 5\%$ for ethene. The GC analyses were performed by MTI's M200 micro GC or a custom modified HP 6890. Since both chromatographs sampled at constant (atmospheric) pressure, they allowed independent calibration for each gas component, including the product aldehyde. Calibrations were based on certified master blends prepared by Scott Specialty Gases or Air Liquide. At the end of the experiment the composition of the catalyst solution and the degree of oxidation of the phosphine ligand were determined by ^{31}P NMR and by GC (HP5890, WCOT Ultimetal with FID detection). The Rh concentration was measured by atomic absorption spectroscopy.

The hydroformylation turnover frequency was calculated as an average from the mass balances for ethene and propanal. The hydrogenation turnover frequency was determined from the rate of formation of ethane.

3. Results and discussions

3.1. Parametric study of reaction variables

The kinetic response to solvents and to changes in the concentration of ethene, Rh, and PPh_3 was first tested in batch reactors. The experiments were carried out at 100°C, and 1000 kPa total pressure with a H_2/CO ratio of one, as described in Section 2.3. The initial partial pressure of ethene in the reactor was between approximately 80 and 160 kPa.

At PPh_3 concentrations higher than approx. 50 mmol/l the turnover frequency vs. ethene conversion plots (Fig. 1) are linear with a zero intercept, suggesting first order kinetics for ethene. Also, since the TOF is independent of [Rh], the reaction is first order in Rh. The ln(1 − conversion) vs. time plots (Fig. 2) are also linear for more than three half lives which is also consistent with a first order in ethene (cf. Section 2.3). The hydroformylation selectivity at these conditions is high, approximately 99.7%. The only other product detected is ethane, forming at 0.2–0.4% selectivity.

Unexpectedly, at low PPh_3 concentrations ($<$ ca. 50 mmol/l) a saturation kinetics can be observed for ethene. As shown in Fig. 3, the data are reproducible. Interestingly, the first order kinetic regime

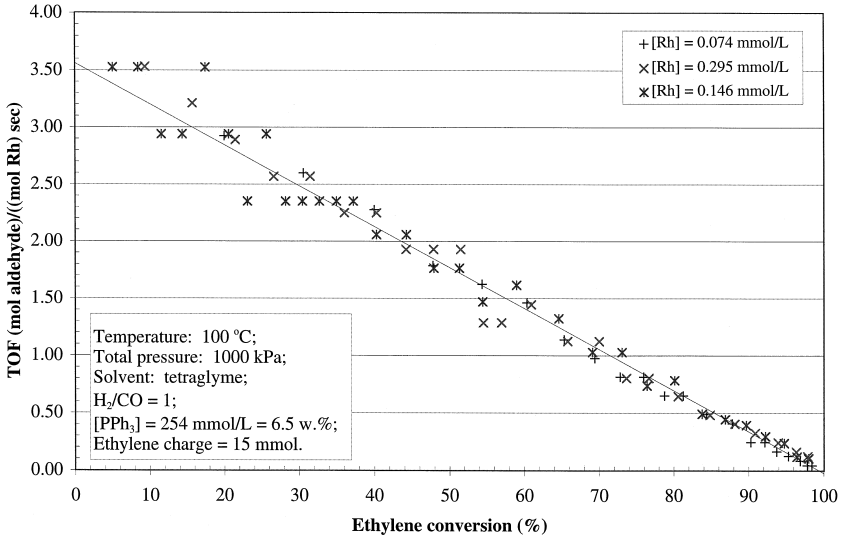

Fig. 1. Hydroformylation rate of ethene as a function of conversion at three different Rh concentrations.

can be expanded to higher ethene concentrations, and the reaction can be accelerated by increasing the H_2/CO ratio in the reactor. Although mass-transfer limitation can lead to similar kinetic response [45], it can be excluded in our experiments because: (I) At the observed maximum gas-uptake rate the calculated gas concentration for all reactants is within 5% of the gas–liquid equilibrium level; and (II) The TOF is independent of the concentration of Rh. Using constant partial pressure of CO, the ethene concentration at which the kinetic saturation occurs becomes lower with lower PPh_3 concentration. The effect of PPh_3 will be discussed later in more detail.

This saturation kinetics in olefin hydroformylation is not without precedent. Thus, saturation, or even substrate inhibition kinetics with Rh/PPh_3 catalyst has also been reported for 1-hexene by Deshpande and Chaudhari [31], for 1-decene by Divekar et al. [29], and for 1-dodecene by Bhanage et

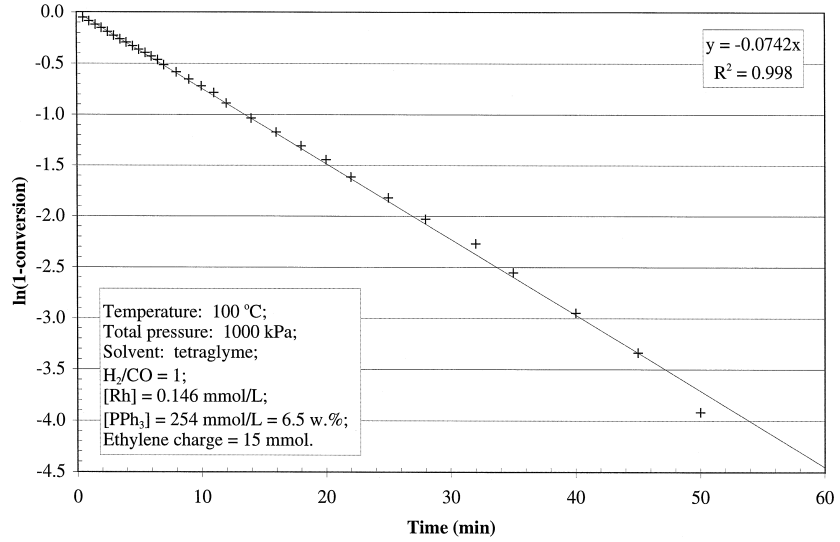

Fig. 2. Integral method plot for the hydroformylation of ethene.

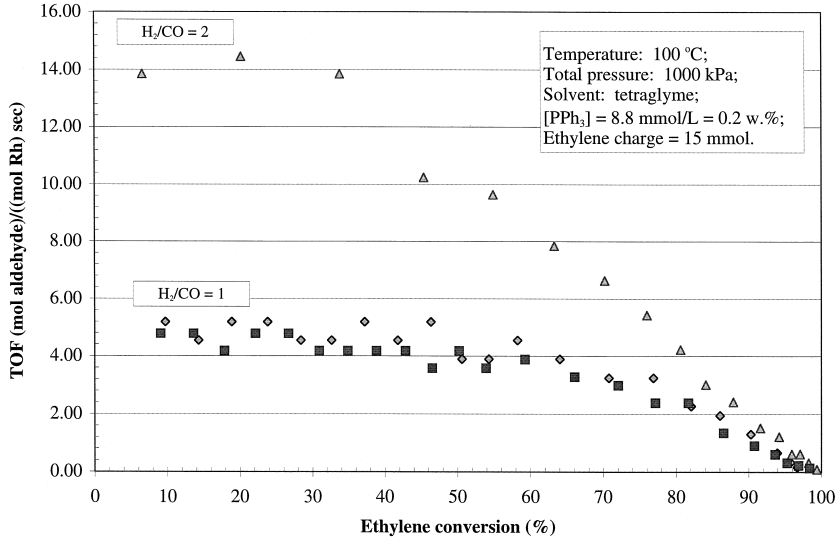

Fig. 3. Saturation kinetics in ethene hydroformylation at low PPh_3 concentrations.

al. [27]. The fractional kinetic order for propylene found by the Montedison group [26] may be the result of an operation in the intermediate kinetic regime. Similar kinetic response has been described by Brown and Wilkinson [6] for the hydroformylation of 1-hexene in benzene at 25°C with $HRh(CO)(PPh_3)_3$, but with no excess PPh_3 present. In their study the maximum TOF does depend on the concentration of Rh. However, at their conditions (no excess ligand) the kinetic order for Rh is less than one, while with excess ligand it is one for a variety of substrates and ligands [15,26–31]. Data obtained in the present study are also consistent with a first order Rh dependence (Fig. 4).

Ethene saturation at low PPh_3 concentrations suggests a rate-limiting step before which there is a quasi-equilibrium involving the olefin. In the dissociative 16/18-electron mechanism proposed by

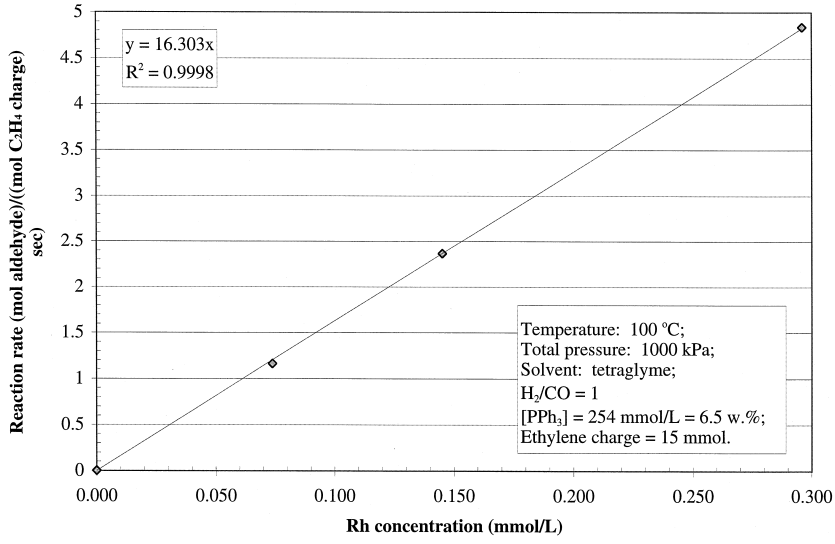

Fig. 4. Hydroformylation rate of ethene as a function of Rh concentration at constant PPh_3 concentration.

Tolman and Faller [1] the earliest such equilibrium step is the formation of $HRh(C_2H_4)(CO)_x(PPh_3)_{3-x}$ ($x = 1–3$) but can also involve the alkyl [$C_2H_5–Rh(CO)_x(PPh_3)_{4-x}$] or acyl [$C_2H_5CO–Rh(CO)_x(PPh_3)_{4-x}$] ($x = 1–4$) intermediates as well. The corresponding rate-limiting steps are olefin and CO insertion or H_2 activation, respectively. Tolman and Faller have proposed [1] that at the saturation limit the rate limiting step is H_2 activation, while at low olefin concentrations the limiting rate is olefin addition to $HRh(CO)_x(PPh_3)_{3-x}$ ($x = 1–2$) or CO dissociation from $HRh(CO)_2(PPh_3)_2$.

The build-up of a non-acyl intermediate has been reported from in situ CIR-FTIR studies of reacting phosphine-modified Rh catalyst systems [20]. The authors have assigned the observed IR-spectrum to an 18-electron alkyl complex. They also proposed [20] that the shift from first to zero order in olefin is due to a shift in the rate-limiting step from CO insertion in the alkyl intermediate to CO dissociation from $HRh(CO)_2(L)_2$ (L = phosphine ligand), which latter complex is the dominating species under typical oxo conditions with Rh/PPh_3. NMR kinetic data [16,17,21], however, make this latter scenario less likely, since it has been found that the dissociation of CO or phosphine is much faster than the rate of catalytic hydroformylation.

Our data support Tolman's proposal regarding a shift in the rate-limiting step. As illustrated by Fig. 5, the turnover frequency is little affected by changes in the H_2/CO ratio at high conversion, i.e., in the ethene first order regime. In contrary, using the same catalyst composition, the reaction rate is increased at low conversion (zero order regime) by increasing the H_2/CO ratio (Fig. 3). Furthermore, a comparison between Figs. 3 and 5 clearly shows that the first order regime expands with increasing phosphine concentration. The changing kinetic response suggests that the rate of hydrogen activation is comparable to the rate of an earlier step in the mechanism. By increasing the rate of hydrogen activation the rate limiting step shifts back to that earlier stage of the catalytic cycle.

Based on the dissociative mechanism of the reaction [1,46] it should be clear that the distribution of Rh intermediates at different $CO/$phosphine ligand ratios, and with it reaction rate and product selectivity, depends on the relative concentrations of CO and PPh_3. At constant partial pressure of CO the determining factor thus becomes the concentration of the phosphine ligand. Our results are in full agreement with this prediction. The data plotted in Fig. 1, for example, show that at the same reaction

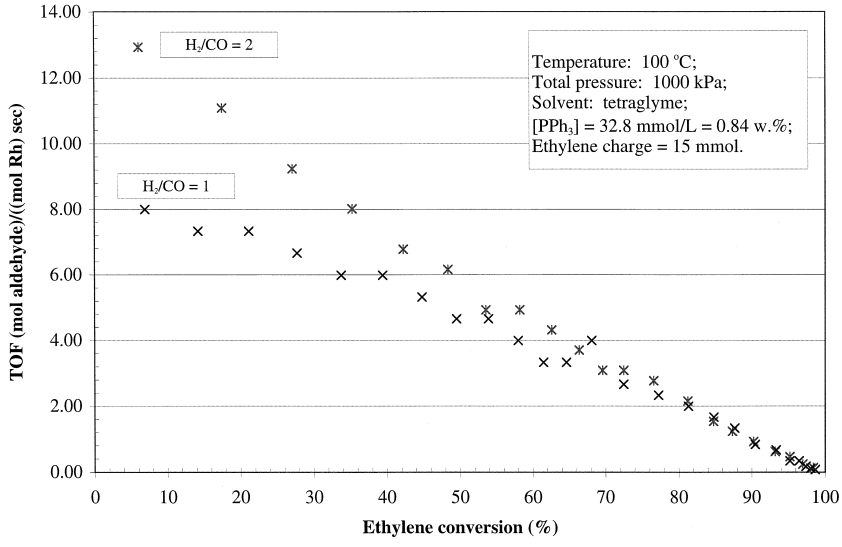

Fig. 5. The effect of H_2/CO ratio in ethene hydroformylation at low PPh_3 concentrations.

condition the TOF/[ethene] is the same as long as the phosphine concentration is the same. This observation is also in agreement with the conclusion of an earlier report by d'Oro et al. [26]. Although it is customary in the hydroformylation literature to report kinetic and selectivity data as a function of the P/Rh ratio [2,32–34], we have not found any correlation between those values when excess phosphine (P/Rh > 3) is present. We have found rather that the TOF/[ethene] values are independent of the P/Rh ratio, and solely depend on the concentration of the phosphine, as long as other reaction variables are constant.

The effect of PPh_3 concentration can be best characterized by defining two regimes depending on the kinetic order of ethene. In the ethene first order regime (high conversion data) the catalytic activity is inhibited by PPh_3 (Fig. 6). At our reaction conditions, as was mentioned earlier, only the first kinetic order regime can be observed for ethene if the phosphine concentration is higher than 0.05 mol/l. The second order rate constant is a monotonous function of the phosphine concentration. From our data, obtained at 80 and 100°C, 270 and 480 kPa of CO, and from 2.5 to 15.0 wt.% PPh_3, the kinetic order for the phosphine is between −0.41 and −0.49. In the hydroformylation of propylene d'Oro et al. [26] reported a similar value, −0.65. In the ethene zero order regime (low ethene conversion), on the other hand, the reaction rate has a maximum at approximately 30 mmol/l phosphine concentration (Fig. 7). A maximum in the reaction rate vs. phosphine concentration function has also been reported for the hydroformylation of propylene [47], 1-hexene [38–40], and *iso*-butene [32]. It has to be mentioned that these literature data represent initial rates and thus were measured at high olefin concentrations. It is therefore quite possible that at low olefin concentrations these olefins, too, would show a monotonous inhibition function for the phosphine.

The positive kinetic response to the phosphine at low phosphine concentrations has been proposed [32] to be due to the break-up of Rh dimers thus providing a higher concentration of the catalytically active mononuclear rhodium hydrides. At high phosphine concentrations the dominating species are mononuclear [1], and the kinetic behavior reflects the trapping of a 16-electron intermediate by the phosphine. It can explain the large shift in the kinetic order of PPh_3 in the low phosphine concentration regime. The mechanistic implications will be discussed in more detail later in Section 3.2.

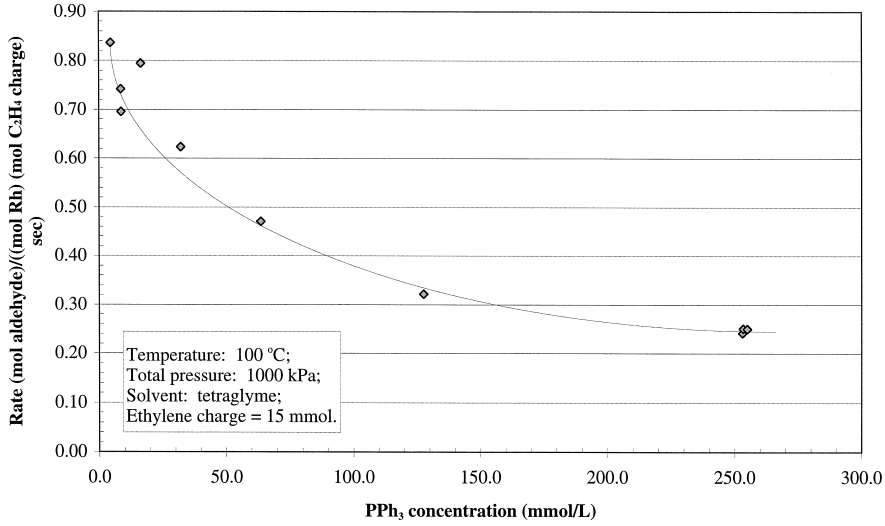

Fig. 6. Catalytic activity as a function of PPh_3 concentration in the first order regime of ethene hydroformylation with Rh/PPh_3 catalyst.

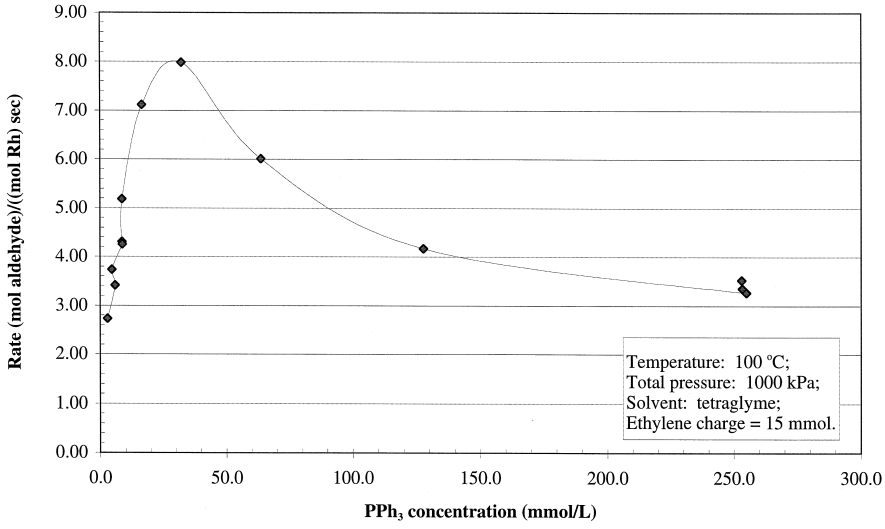

Fig. 7. Maximum observed rate as a function of PPh_3 concentration in ethene hydroformylation with Rh/PPh_3 catalyst.

The kinetic effect of CO and H_2 was investigated in continuous-flow reactors as described in Section 2.4. In these experiments all other variables were kept constant, while the partial pressure of either CO or H_2 was changed using methane as an inert balance to maintain constant pressure.

As shown in Fig. 8, the kinetic order for CO is positive in a narrow range of low CO partial pressures but it becomes negative after going through a maximum reaction rate. Similar kinetic response to CO has been reported for the hydroformylation of 1-hexene [39], 1-octene [28], 1-decene [29], and 1-dodecene [27] with $HRh(CO)(PPh_3)_3$ catalyst. It should be noticed on Fig. 8, that the position of the maximum on the CO partial pressure axis, and the rate response to the same Δp_{CO} is a function of the PPh_3 concentration. Namely, the maximum is shifted toward higher p_{CO} values at higher PPh_3 concentrations, while the rate sensitivity toward p_{CO} changes in the opposite direction.

It is known [1,3–6,17,18] that under hydroformylation conditions the dominating Rh-hydride component is $HRh(CO)_2(PPh_3)_2$, and both CO and PPh_3 undergo rapid exchange [17,18] via the

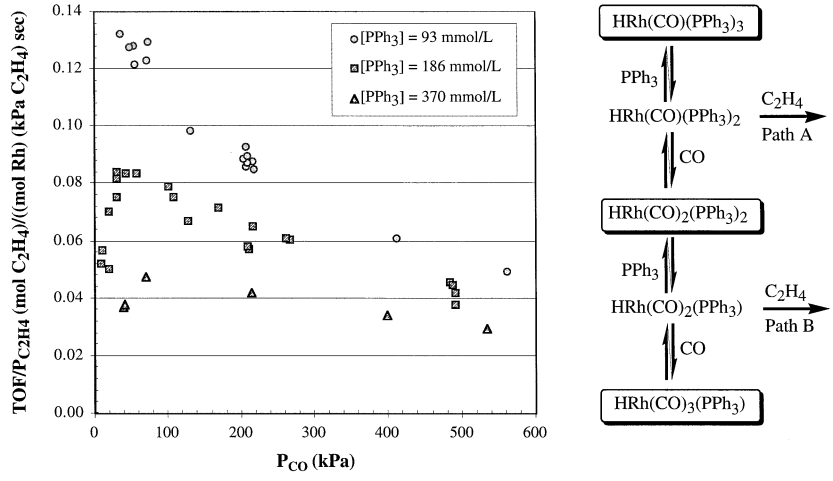

Fig. 8. The effect of CO on the hydroformylation rate of ethene at different PPh_3 concentrations.

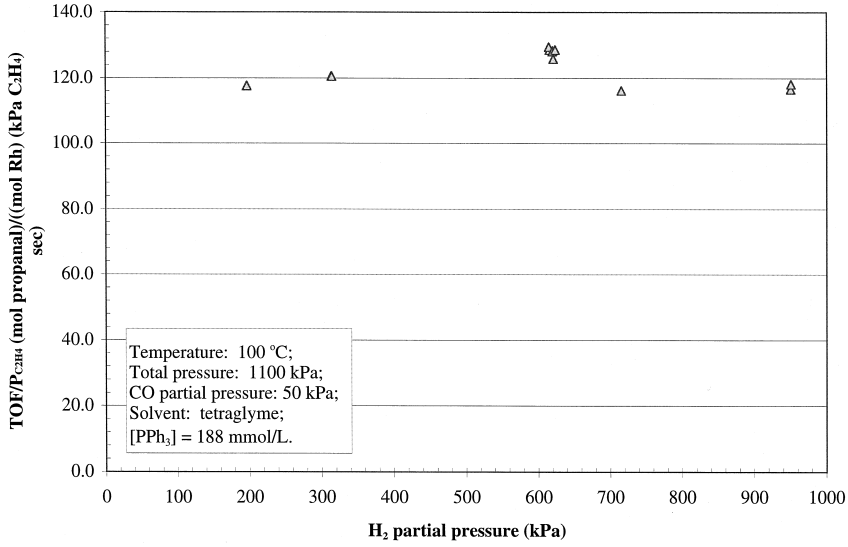

Fig. 9. The effect of H_2 partial pressure on the hydroformylation rate of ethene with Rh/PPh_3 catalyst.

corresponding 16-electron intermediates, $HRh(CO)(PPh_3)_2$ and $HRh(CO)_2(PPh_3)$, respectively. These two coordinatively unsaturated species are believed to be the entry points of the two prevalent kinetic paths in the phosphine-modified Rh hydroformylation of olefins (depicted as Path A and B in Fig. 8). They can be trapped by CO or PPh_3 and driven back to the corresponding coordinatively saturated hydrides, or bind an ethene molecule, initiating a catalytic cycle. The relative concentration of the two 16-electron intermediates, and thus their contribution to olefin conversion, is a function of the PPh_3/CO ratio. The overall rate is a linear combination of the rates of the two parallel paths. It will be shown later that the observed kinetic response to CO can be reconciled with the above mechanism.[1]

At high PPh_3 concentrations, i.e., in the ethene first order regime, the hydroformylation rate is not affected by changing hydrogen partial pressure (Fig. 9). The rate-limiting step in the hydroformylation of ethene therefore must be prior to H_2 activation. The rate of ethene hydrogenation at the same conditions, on the other hand, shows a first order dependence on the partial pressure of H_2 (Fig. 10).

Literature data regarding the kinetic order of H_2 in the hydroformylation of olefins may seem contradicting. Thus, a detailed study of propylene hydroformylation with Rh/PPh_3 catalyst ($P/Rh > 3$) concluded that the kinetic order for H_2 is essentially zero [26]. Brown and Wilkinson [6], however, reported first order for the hydroformylation of 1-hexene with $HRh(CO)(PPh_3)_3$ at low catalyst concentration, and a positive but decreasing order at higher catalyst concentration. A similarly changing kinetic order was also reported for 1-decene [29] and allyl alcohol [30], while first order was published for 1-hexene [31] and 1-dodecene [27] with the same catalyst. Invariably, in all studies the kinetic order of H_2 is higher than zero when the PPh_3 concentration is low and tends to zero when the

[1] Note: Although there are four possible conversion paths starting with the corresponding 16-electron complexes with a general formula of $HRh(CO)_x(PPh_3)_{3-x}$ ($x = 0–3$) [1], based on published equilibrium data [1] and our kinetic analysis (cf. Chapter 3.2) we propose that only the routes shown in Fig. 8 will contribute to any significant degree, and the other two paths are negligible under the conditions of our investigation.

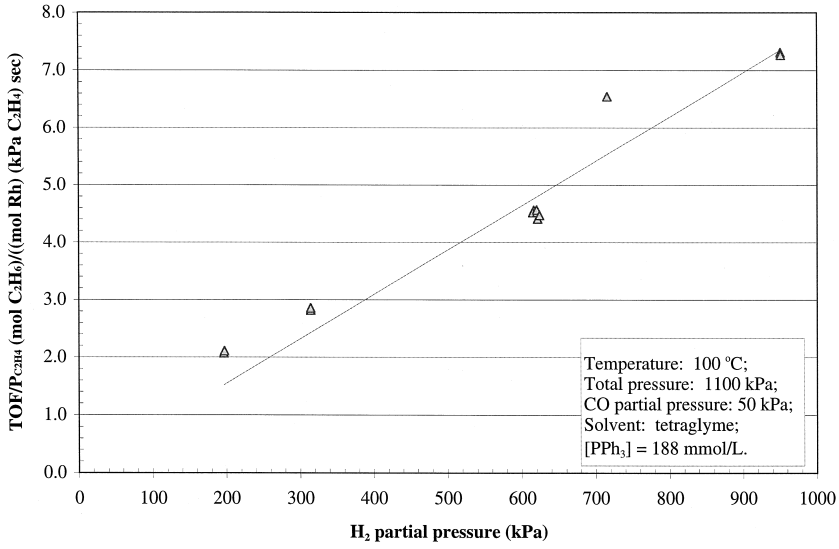

Fig. 10. The effect of H_2 partial pressure on the hydrogenation rate of ethene with Rh/PPh_3 catalyst.

phosphine concentration is high. In our experiments, covering a wide range of PPh_3 concentrations, the kinetic orders for both ethene and H_2 are dependent on the concentration of PPh_3 (cf. Figs. 3 and 5, and discussion on the effect of ethene). The mechanistic implications will be discussed in Section 3.2.

The hydroformylation rates of ethene in toluene, tetraglyme, dioctyl phthalate, Texanol, and isoamyl butyrate at 100°C, 1 MPa CO/H_2 (1:1), 5 wt.% PPh_3 are nearly the same. The reaction rates measured in *n*-butanal and propanal at 80°C, 1 MPa CO/H_2 (1:1), 5 wt.% PPh_3, on the other hand, are significantly different from that of measured in tetraglyme, and have a ratio of 0.73:0.56:1, respectively. Literature reports suggest increased rates when the solvent is changed from non-polar

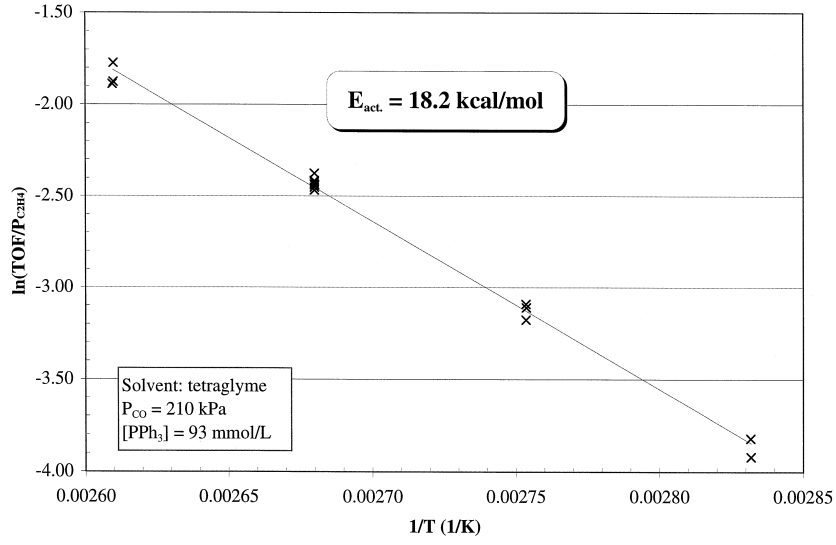

Fig. 11. Temperature effect in the hydroformylation of ethene with Rh/PPh_3 catalyst.

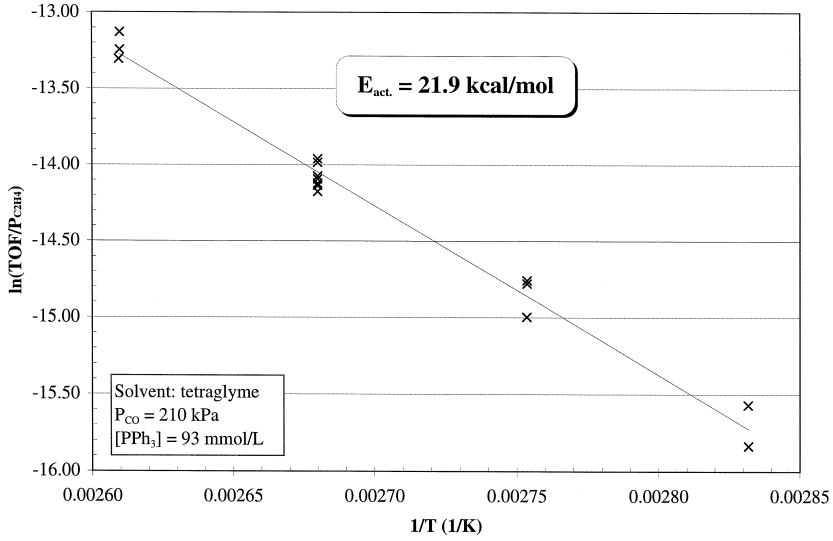

Fig. 12. Temperature effect in the hydrogenation of ethene with Rh/PPh_3 catalyst.

hydrocarbons to oxygenates. Thus, in the hydroformylation of propylene the product butanal has been reported [42] to increase the reaction rate in benzene. We did not observe similar effect in the batch hydroformylation of ethene or propylene in toluene. Substantial solvent effects have also been reported in the hydroformylation of allyl alcohol [35] and 1-octene [33]. The later two papers suggest metal–solvent interactions. In our study we have not found spectroscopic evidence for solvent coordination to the metal.

The effect of temperature on the rate of hydroformylation (Fig. 11) and hydrogenation (Fig. 12) of ethene was tested in tetraglyme between 80 and 110°C at 210 kPa partial pressure of CO and 93 mmol/l concentration of PPh_3. The kinetic data for both reactions were obtained from the same CSTR experiments. The activation energy for hydroformylation has been found to be lower (18.2 kcal/mol) than for hydrogenation (21.9 kcal/mol). The activation energy for ethene hydroformylation obtained from batch experiments at 460 kPa CO and 180–360 mmol/l PPh_3 concentration is somewhat higher, 19.1 ± 0.2 kcal/mol, but increasing ethane selectivity at higher temperatures indicates higher activation energy for hydrogenation than for hydroformylation in the batch results, as well. Literature values for the activation energy in the hydroformylation of olefins scatter considerably. The 20.6 and 19 kcal/mol reported for propylene [26,48] and 22 kcal/mol for 1-butene [16] are relatively close to our values. Bhanage et al. [27], Divekar et al. [29] and Deshpande and Chaudhari [31], however, published activation energies ranging from 11.8 to 28 kcal/mol for the hydroformylation of 1-hexene, 1-decene, and 1-dodecene. Their data were obtained from empirical fits of the experimental data, thus the activation energies can be model dependent, which may explain their wide variance and some of the unusually low values.

3.2. Kinetic model for the hydroformylation and hydrogenation of ethene

The database for the kinetic model development was generated in CSTR experiments as described in Section 2.4. The range of operating conditions covered in these continuous-flow runs is given in Table 1. The kinetic data are summarized in the Appendix A.

Table 1
Process variable ranges in the kinetic model database for the hydroformylation of ethene with Rh/PPh_3 catalyst in tetraglyme

Variable	Minimum	Maximum
Temperature (°C)	80.0	110.0
CO partial pressure (kPa)	8.1	562.0
H_2 partial pressure (kPa)	287.0	747.0
C_2H_4 partial pressure (kPa)	7.2	37.8
CH_4 (as inert balance) partial pressure (kPa)	55.5	853
Total reactor pressure (kPa)	1100	1252
PPh_3 concentration (mmol/l)	93	372
Rh concentration (mmol/l)	0.058	0.932

3.2.1. Kinetic model for ethene hydroformylation

As we discussed in Section 3.1, all of our kinetic observations can be reconciled with a refined Wilkinson mechanism in which two parallel catalytic cycles are initiated by the coordination of ethene to the 16-electron hydrides with the general formula of $HRh(CO)_x(PPh_3)_{3-x}$, ($x = 1$ or 2). We have excluded the two extreme combinations ($x = 0$ and 3) since their concentrations at our conditions are expected to be much lower than for $x = 1$ or 2, and there is no reason to assume that they would significantly contribute to the conversion of ethene. It can be shown, however, that the form of the kinetic expression would not be different for any other neighboring combinations (i.e., 0 and 1 or 2 and 3). Furthermore, since it is reasonable to assume that energetically the associative route would be strongly disfavored over the dissociative path, only the latter is considered. Indeed, in agreement with literature analyses [1,2], we have found that the kinetics of ethene hydroformylation can be described satisfactorily without invoking the associative route.

In accounting for the Rh in solution, we can assume that only the coordinatively saturated components are present in significant concentrations, and all other species are negligible. NMR results indicate [14,16] that the concentration of binuclear Rh complex(es) is also low at the reaction conditions of the present study. In fact, the vast majority of Rh is present as $HRh(CO)_x(PPh_3)_{4-x}$, where $x = 1$ or 2. The 16-electron initiators of the catalytic cycles are formed by the dissociation of CO or PPh_3 from these 18-electron complexes.

In our kinetic analysis we have considered four possible rate-limiting steps: H_2 activation (Eq. (11)), CO insertion (Eq. (12)), ethene insertion (Eq. (13)), and ethene addition (Eq. (14)).

$$C_2H_5CO{-}Rh(CO)_x(PPh_3)_{3-x} + H_2 \rightarrow C_2H_5{-}COH + HRh(CO)_x(PPh_3)_{3-x}, \qquad x = 1 \text{ or } 2 \tag{11}$$

$$C_2H_5{-}Rh(CO)_x(PPh_3)_{4-x} \rightarrow C_2H_5CO{-}Rh(CO)_{x-1}(PPh_3)_{4-x}, \qquad x = 2 \text{ or } 3 \tag{12}$$

$$HRh(C_2H_4)(CO)_x(PPh_3)_{3-x} \rightarrow C_2H_5{-}Rh(CO)_x(PPh_3)_{3-x}, \qquad x = 1 \text{ or } 2 \tag{13}$$

$$HRh(CO)_x(PPh_3)_{3-x} + C_2H_4 \rightarrow HRh(C_2H_4)(CO)_x(PPh_3)_{3-x}, \qquad x = 1 \text{ or } 2 \tag{14}$$

As we mentioned earlier, the initiation of the catalytic cycle by the dissociation of CO or PPh_3 from $HRh(CO)_x(PPh_3)_{4-x}$ ($x = 1$–3) should not be rate-limiting since it has been found to be fast on the time scale of hydroformylation [16,17,21].

At high PPh_3 concentrations, i.e., at the conditions of our modeling study, the kinetic order for H_2 is zero, thus the rate-limiting step has to be prior to H_2 activation. We have also rejected CO insertion as the rate-limiting step, since it could not be reconciled with a negative kinetic order for CO. The rate-determining step therefore is either the addition or the insertion of ethene (Eqs. (14) and (13),

respectively). Our kinetic data cannot resolve the two reactions but, as will be shown later, it does not affect the final form of the kinetic model since it is the same for both scenarios. For further analysis ethene insertion is chosen as a rate-determining step. This choice will conveniently allow the discussion of both cases and will not influence the final results.

The mechanism derived from the previous analysis is depicted in Scheme 2. The scheme includes a Rh-dimer to show how H_2 can increase the concentration of the catalytically active mononuclear Rh-species. However, since the process-variable range covered in our modeling database falls into the zero order regime for H_2, the concentration of these dimers must be negligible and therefore they are not included in the Rh-balance. The total Rh in solution therefore can be accounted for by five mononuclear 18-electron complexes, $HRh(CO)_x(PPh_3)_{4-x}$ ($x = 1$–3), and $HRh(C_2H_4)(CO)_x(PPh_3)_{3-x}$ ($x = 1$ or 2). These complexes are at equilibrium via rapid exchange of C_2H_4, CO, and PPh_3. The Rh-species reacting in the rate-determining step are $HRh(C_2H_4)(CO)_2(PPh_3)$ or $HRh(C_2H_4)(CO)(PPh_3)_2$. Since the k_1 and k_2 paths are parallel, the overall rate is the sum of two rates. This mechanism yields the following rate expression for ethene hydroformylation:

$$\mathrm{TOF} = \frac{k_1 K_1 K_{11} \dfrac{p_{C_2H_4}}{[PPh_3]} + k_2 K_2 K_{21} \dfrac{p_{C_2H_4}}{p_{CO}}}{1 + K_1 K_{11} \dfrac{p_{C_2H_4}}{[PPh_3]} + K_1 K_0 \dfrac{p_{CO}}{[PPh_3]} + K_2 K_3 \dfrac{[PPh_3]}{p_{CO}} + K_2 K_{21} \dfrac{p_{C_2H_4}}{p_{CO}}} \tag{15}$$

where K_0, K_1, K_2, K_3, K_{11}, and K_{21} are equilibrium constants and k_1 and k_2 are rate constants.

Since all reactions take place in the liquid phase, the equilibrium constants will implicitly contain the vapor–liquid equilibrium proportionality (Henry's coefficient) for each of the gaseous components. These Henry's coefficients are assumed to be independent of the gas phase composition.

It should be noticed that at high ethene and low PPh_3 or CO concentrations Eq. (15) leads to zero order in ethene, which has been observed experimentally for the high ethene/low PPh_3 case (cf. Chapter 3.1). However, the conditions of the modeling database cover the ethene first order kinetic regime only and the analysis will be limited to this region. At these conditions the concentration of

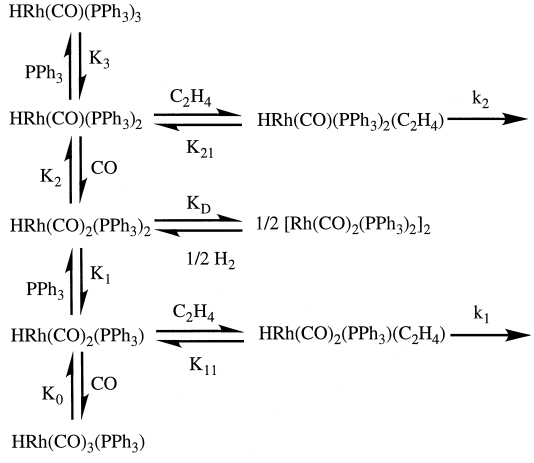

Scheme 2. Mechanism for ethene hydroformylation with Rh/PPh_3 catalyst.

the ethene complexes $HRh(C_2H_4)(CO)_x(PPh_3)_{3-x}$ ($x = 1$ or 2) must be low and, in turn, the ethene-containing terms in the denominator are negligible. Furthermore, the lack of equilibrium data does not allow the resolution of the individual equilibrium constants. Eq. (15) therefore can be simplified to Eq. (16):

$$\mathrm{TOF} = \frac{k_1' \dfrac{p_{C_2H_4}}{[PPh_3]} + k_2' \dfrac{p_{C_2H_4}}{p_{CO}}}{1 + K_1' \dfrac{p_{CO}}{[PPh_3]} + K_2' \dfrac{[PPh_3]}{p_{CO}}} \tag{16}$$

where $k_1' = k_1 K_1 K_{11}$, $k_2' = k_2 K_2 K_{21}$, $K_1' = K_1 K_0$, and $K_2' = K_2 K_3$. It can be easily shown that the final kinetic expression would be the same as Eq. (16) if the rate-determining step were ethene-addition, as well.

The four constants in Eq. (16), k_1', k_2', K_1', K_2', have been regressed using all data (44 data points) in the modeling database at 100°C. The results from three regression cases ($k_1' = 0$; $k_2' = 0$; and k_1', $k_2' \neq 0$) are shown in Table 2.

The regression results suggest that the dominating conversion path is k_1'. Without the k_1' term (Case 1) the standard error is high, and the equilibrium constant K_1' is negative. The k_1' route alone (Case 2) gives an excellent fit. The inclusion of k_2' (Case 3) brings no improvement in the standard error, and results in a non-physical, negative value for k_2'. Thus it is justifiable to assume that k_2' is 0. Mechanistically, this implies that the main pathway for ethene hydroformylation is through the $HRh(C_2H_4)(CO)_2(PPh_3)$ intermediate, and the contribution of the path through $HRh(C_2H_4)(CO)(PPh_3)_2$ is negligible. The final kinetic expression therefore simplifies to:

$$\mathrm{TOF} = \frac{k_1' \dfrac{p_{C_2H_4}}{[PPh_3]}}{1 + K_1 \dfrac{p_{CO}}{[PPh_3]} + K_2' \dfrac{[PPh_3]}{p_{CO}}} \tag{17}$$

The experimental data and the fit by the above kinetic model are shown in Fig. 13, where the average error is 7.6%. Eq. (17) is first order in $p_{C_2H_4}$ and [Rh], zero order in p_{H_2}, monotonously decreasing with $[PPh_3]$ and has a maximum with respect to p_{CO}. The model therefore correctly describes the kinetic correlations observed experimentally (cf. Section 3.1).

3.2.2. Kinetic model for hydrogenation selectivity in ethene hydroformylation

In the kinetic analysis of hydroformylation we have concluded that the rate-determining step either is, or preceeds the formation of a 16-electron alkyl intermediate (see Scheme 2). That 16-electron

Table 2
Regression results for Eq. (16) using CSTR data for ethene hydroformylation with Rh/PPh_3 catalyst at 100°C

	k_1'	k_2'	K_1'	K_2'	$\Sigma(\mathrm{error})^2$
Case 1	0	7.68	−0.000345	396.0	80.9
Case 2	0.0176	0	0.000496	31.8	0.409
Case 3	0.0173	−0.318	0.000473	2.53	0.401

TOF in (mol aldehyde)/(mol Rh s).
$[PPh_3]$ in mol/l.
Pressures in kPa.

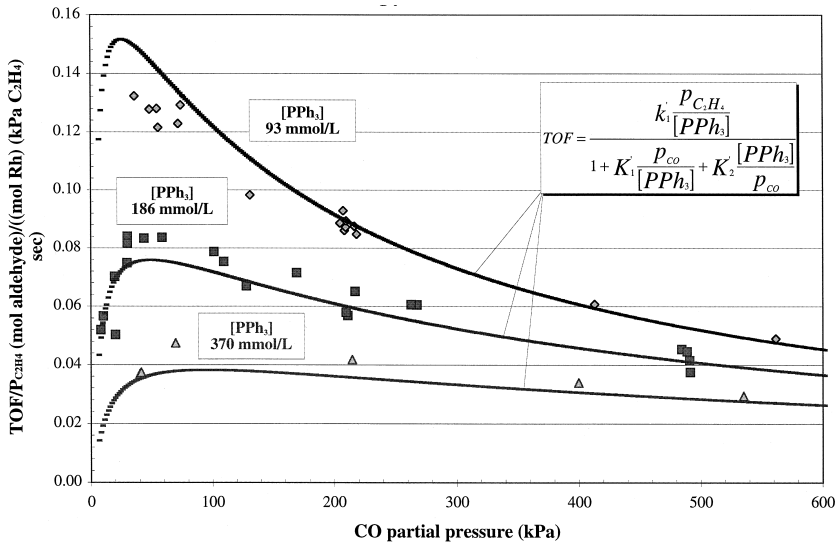

Fig. 13. Model fit for the hydroformylation of ethene with Rh/PPh$_3$ catalyst in tetraglyme at 100°C.

intermediate can react with CO, PPh$_3$, or H$_2$. The former two reactions would yield acyl-intermediates after CO insertion, and ultimately lead to the formation of the aldehyde (Scheme 1). The addition of H$_2$ to the coordinatively unsaturated alkyl intermediate, on the other hand, will yield ethane. Therefore the hydroformylation vs. hydrogenation selectivity is determined by the competition of CO and PPh$_3$ vs. H$_2$ for the unsaturated alkyl intermediate.

Scheme 3 depicts all possible routes leading to propanal and ethane. There are two branching points between hydroformylation and hydrogenation. Based on our previous discussions, however, only the route via k_1 needs to be considered, since that is the dominating path under the conditions of this study (cf. Section 3.2.1). By this mechanism the rate of hydrogenation should be first order in H$_2$, and indeed, that is what was found experimentally (see Fig. 10). Furthermore, the hydrogenation vs.

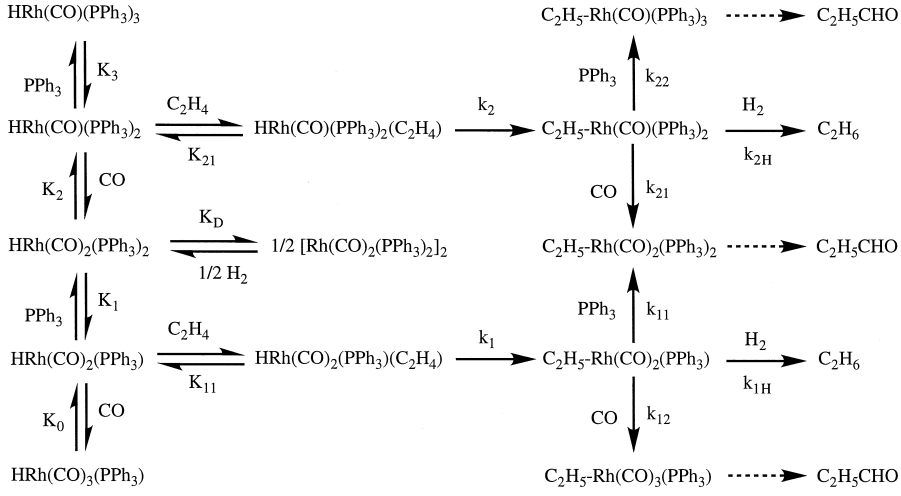

Scheme 3. Mechanism for ethene hydrogenation under hydroformylation conditions with Rh/PPh$_3$ catalyst.

hydroformylation selectivity is expected to be the function of the relative concentrations of H_2 vs. CO and PPh_3, as shown by Eq. (18):

$$\frac{\mathrm{TOF}_{C_2H_6}}{\mathrm{TOF}_{C_2H_5CHO}} = \frac{p_{H_2} k_{1H}}{p_{CO} k_{12} + [PPh_3] k_{11}} \tag{18}$$

Experimentally, ethane selectivity is found to be a linear function of p_{H_2}/p_{CO} and independent of the concentration of PPh_3 (Fig. 14). It suggests that the hydrogenation vs. hydroformylation selectivity is determined by the competition between H_2 and CO (k_{1H} vs. k_{12} route), and can be simply expressed as:

$$\frac{\mathrm{TOF}_{C_2H_6}}{\mathrm{TOF}_{C_2H_5CHO}} = k' \frac{p_{H_2}}{p_{CO}} \tag{19}$$

The regressed value for k' at 100°C is 0.00202, and Eq. (19) provides an excellent fit over more than two orders of magnitude.

3.2.3. Temperature effects

At temperatures other than 100°C, there are not enough data available for a full regression of Eq. (17) to determine the temperature dependence of the equilibrium constants, K_1' and K_2'. However, since the heat of reaction for the CO/PPh_3 ligand-exchange is expected to be small, and the gas solubilities are not strongly temperature dependent, K_1' and K_2' probably are not strong functions of temperature. Assuming therefore that K_1' and K_2' are not temperature dependent will likely give an acceptable fit. Applying the above approximation in a regression of all the data in the Appendix yields activation energies of 17.0 kcal/mol for hydroformylation and 20.4 kcal/mol for hydrogenation. These values are indeed not much different from the ones obtained experimentally at constant

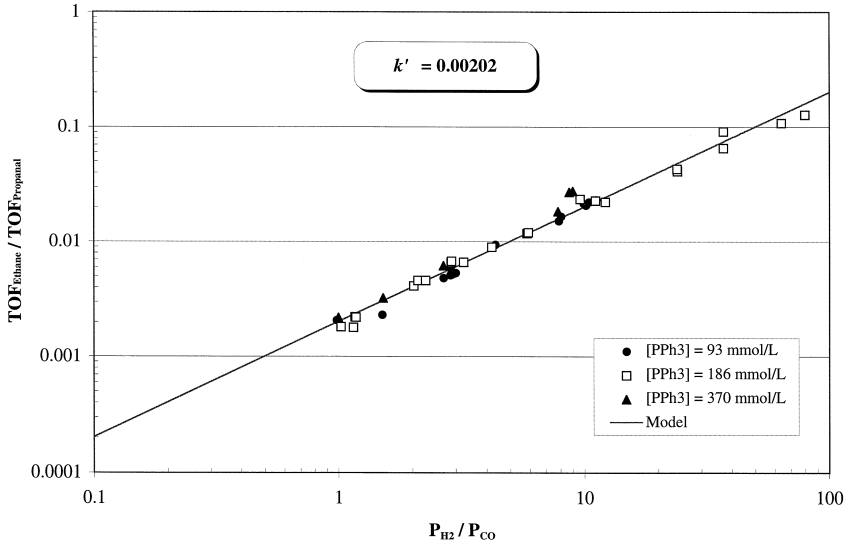

Fig. 14. Model fit for the hydrogenation vs. hydroformylation selectivity of ethene with Rh/PPh_3 catalyst at 100°C.

CO/PPh_3 ratios (see Chapter 3.1). The hydroformylation rates and hydrogenation selectivities at other than 100°C thus can be calculated as follows:

$$TOF^{T}_{Propanal} = \frac{0.0176e^{\frac{17000}{1.987}\left(\frac{1}{373}-\frac{1}{T}\right)}\frac{p_{C_2H_4}}{[PPh_3]}}{1 + 0.000496\frac{p_{CO}}{[PPh_3]} + 31.8\frac{[PPh_3]}{p_{CO}}} \quad (20)$$

and

$$\frac{TOF_{Ethane}}{TOF_{Propanal}} = 0.00202e^{\frac{3400}{1.987}\left(\frac{1}{373}-\frac{1}{T}\right)}\frac{p_{H_2}}{p_{CO}} \quad (21)$$

TOF is in (mol product)/(mol Rh s), pressures are in kPa, and $[PPh_3]$ is in mol/l.

4. Conclusions

The kinetics of ethene hydroformylation with Rh/PPh_3 catalyst ($P/Rh > 3$) is first order in rhodium. The kinetic order for ethene is also one at the industrially important conditions, when the PPh_3 concentration is relatively high (> 50 mmol/l). However, the combination of low phosphine and high olefin concentration leads to a saturation in ethene. The kinetic effect of the CO and PPh_3 ligands is also a function of their concentration: both inhibit the reaction above a threshold value, below which a positive fractional order can be observed. Hydrogen has little effect on the rate of hydroformylation in the ethene first order kinetic regime. It does have an effect, however, when ethene saturation occurs: increasing hydrogen pressure increases the reaction rate by expanding the ethene first order regime. This phenomenon may be linked to a shift in the rate determining step of the reaction. Activation energies obtained at constant PPh_3/CO ratios range between 18.2 and 19.1 kcal/mol for hydroformylation and 22 kcal/mol for hydrogenation.

Under typical hydroformylation conditions the selectivity for propionaldehyde is nearly 100%. The olefin hydrogenation selectivity is low (approximately 0.2–0.4 mol%) and can be described by a linear function of the p_{H_2}/p_{CO} ratio. Ethane selectivity increases with increasing temperature, indicating that the activation energy for olefin hydrogenation is higher than hydroformylation. The aldehyde hydrogenation selectivity is very low. Propanol can only be detected in long term CSTR runs.

Our kinetic data suggest that the rate-determining step in the ethene first order regime is olefin addition or olefin insertion. Based on a refined Wilkinson mechanism [1], a kinetic model has been developed to predict the rates of ethene hydroformylation and hydrogenation. In this model the hydrogenation vs. hydroformylation selectivity is determined by the competition of H_2 vs. CO for a 16-electron alkyl intermediate in a post-rate-determining step. The model has proved to be very accurate even at operating conditions which are outside of its database.

Acknowledgements

The authors would like to thank the management of Exxon Research and Engineering and Exxon Chemical for their support. We would also like to thank Dr. Roy L. Pruett and Dr. Harry W. Deckman for the many useful discussions.

Appendix A. Continuous flow kinetic data for the hydroformylation of ethene with Rh/PPh_3 catalyst in tetraglyme

Temperature	Liquid concentration		Total pressure	Partial pressures in the reactor						TOF	
	Rh	PPh_3		CO	H_2	CH_4	C_2H_4	C_2H_6	Propanal	C_2H_6	Propanal
°C	mmol/l	mmol/l	kPa abs	kPa	kPa	kPa	kPa	kPa	kPa	(mol product)/((mol Rh) s)	
80.0	0.234	94	1234	211.2	598.8	382.3	20.1	0.08	21.7	0.0016	0.3982
80.0	0.118	94	1227	213.6	596.0	376.8	25.5	0.07	15.3	0.0026	0.5594
90.0	0.117	94	1222	223.7	595.8	338.8	30.6	0.14	32.9	0.0053	1.3302
90.0	0.059	94	1231	213.7	596.2	379.5	26.0	0.08	15.8	0.0060	1.1586
90.0	0.924	189	1105	30.6	495.9	522.3	14.7	1.14	40.3	0.0173	0.6215
90.0	0.926	189	1105	103.5	500.0	444.8	17.5	0.34	38.7	0.0050	0.5895
90.0	0.927	190	1105	206.8	504.4	336.8	19.8	0.15	37.0	0.0021	0.5901
90.0	0.930	190	1105	489.8	499.9	57.8	24.2	0.05	33.4	0.0006	0.4893
90.0	0.932	191	1105	486.7	506.6	55.5	25.0	0.06	31.1	0.0006	0.4991
90.0	0.932	191	1105	486.3	506.7	56.2	24.6	0.06	31.1	0.0006	0.4703
90.0	0.117	94	1227	209.3	595.6	381.0	18.4	0.11	23.0	0.0042	0.8339
90.0	0.233	93	1235	207.3	598.3	387.0	13.0	0.13	29.6	0.0024	0.5430
100.0	0.146	185	1249	30.0	717.4	453.8	11.4	1.37	35.4	0.0392	0.9544
100.0	0.146	185	1249	30.0	716.4	454.9	11.7	1.43	34.9	0.0408	0.9495
100.0	0.147	186	1247	8.2	650.0	545.7	12.4	3.45	27.7	0.0820	0.6429
100.0	0.146	186	1247	109.3	645.3	446.9	12.3	0.39	33.2	0.0111	0.9252
100.0	0.147	186	1244	209.8	605.1	387.5	13.8	0.18	27.9	0.0054	0.7983
100.0	0.059	94	1229	209.7	596.7	381.4	18.9	0.13	22.5	0.0097	1.6447
100.0	0.146	185	1247	19.5	720.3	459.0	12.6	2.04	33.7	0.0578	0.8864
100.0	0.127	93	1221	54.4	551.3	573.8	9.7	0.65	31.1	0.0257	1.2381
100.0	0.127	93	1222	218.6	585.1	373.5	13.8	0.16	30.9	0.0056	1.1696
100.0	0.127	93	1222	71.9	576.2	533.3	9.5	0.51	30.7	0.0195	1.1698
100.0	0.116	93	1238	207.6	600.2	387.7	12.2	0.16	30.4	0.0062	1.1313
100.0	0.116	93	1223	208.6	602.5	353.2	18.8	0.22	39.7	0.0083	1.6162
100.0	0.127	93	1221	48.4	539.2	594.0	9.4	0.67	29.3	0.0278	1.2023
100.0	0.127	93	1223	55.6	551.5	576.7	9.4	0.61	29.2	0.0245	1.1448
100.0	0.127	93	1222	73.9	580.3	529.0	9.3	0.48	29.0	0.0182	1.2016

100.0	0.127	93	1223	412.9	621.8	142.6	16.9	0.08	28.6	0.0024	1.0268
100.0	0.127	93	1223	131.1	569.6	482.9	11.3	0.27	27.8	0.0104	1.1062
100.0	0.116	93	1224	216.7	616.3	339.2	16.3	0.20	35.4	0.0073	1.4267
100.0	0.128	94	1222	561.9	552.0	67.1	17.9	0.04	23.1	0.0018	0.8763
100.0	0.117	94	1220	204.8	612.7	356.1	14.4	0.19	31.9	0.0068	1.2740
100.0	0.117	94	1221	209.9	624.2	343.2	13.4	0.18	30.2	0.0063	1.1981
100.0	0.129	94	1221	36.0	374.9	783.2	8.6	0.42	18.0	0.0251	1.1361
100.0	0.174	183	1226	29.9	286.7	852.6	11.5	1.10	44.2	0.0202	0.8593
100.0	0.175	185	1235	491.5	565.0	125.5	12.8	0.09	40.1	0.0009	0.4806
100.0	0.176	185	1217	484.3	565.2	120.3	14.9	0.08	32.2	0.0015	0.6756
100.0	0.176	185	1226	169.2	546.5	464.3	13.7	0.23	31.9	0.0065	0.9787
100.0	0.177	186	1222	267.6	542.3	365.7	15.4	0.14	30.8	0.0038	0.9319
100.0	0.177	186	1235	490.9	578.4	119.7	15.0	0.08	30.8	0.0014	0.6243
100.0	0.177	186	1226	262.9	553.3	367.6	13.7	0.13	28.4	0.0038	0.8272
100.0	0.467	188	1100	127.9	536.7	371.9	16.5	0.44	46.6	0.0098	1.1042
100.0	0.468	188	1100	43.6	484.2	514.8	13.8	1.04	42.5	0.0262	1.1535
100.0	0.470	189	1100	217.2	491.5	337.8	15.6	0.20	37.8	0.0046	1.0143
100.0	0.472	190	1100	488.8	499.4	59.2	18.9	0.07	33.6	0.0015	0.8421
100.0	0.127	367	1221	69.6	543.7	547.8	26.9	0.60	32.4	0.0233	1.2776
100.0	0.127	367	1223	399.9	608.2	147.1	35.9	0.12	31.8	0.0039	1.2129
100.0	0.128	368	1221	214.9	574.4	371.9	28.8	0.21	30.8	0.0073	1.1983
100.0	0.129	371	1222	535.4	535.0	95.3	33.5	0.06	22.6	0.0021	0.9823
100.0	0.129	372	1221	40.2	360.6	779.9	23.1	0.38	16.8	0.0234	0.8499
100.0	0.129	372	1222	41.5	359.0	781.4	23.0	0.38	16.7	0.0231	0.8574
100.0	0.147	187	1247	20.3	746.8	437.4	13.1	2.12	27.6	0.0597	0.6589
100.0	0.144	183	1240	101.4	591.1	486.3	12.8	0.54	48.1	0.0118	1.0045
100.0	0.146	185	1246	58.7	714.0	426.8	12.0	0.74	34.1	0.0222	1.0018
100.0	0.147	186	1248	10.2	653.0	539.8	12.1	3.08	30.0	0.0740	0.6852
100.0	0.147	186	1252	211.2	607.4	391.0	14.1	0.18	28.4	0.0052	0.8008
110.0	0.115	93	1223	206.7	608.8	352.2	11.6	0.33	43.3	0.0125	1.7764
110.0	0.058	93	1232	206.7	598.1	385.2	12.6	0.20	29.4	0.0150	2.1430
110.1	0.116	92	1229	203.0	594.2	386.8	8.7	0.23	36.4	0.0086	1.3129

References

[1] C.A. Tolman, J.W. Faller, Mechanistic studies of catalytic reactions using spectroscopic and kinetic techniques, in: L.H. Pignolet (Ed.), Homogeneous Catalysis with Metal Phosphine Complexes, Plenum, New York, 1983.
[2] C.D. Frohning, Ch. W. Kohlpaintner, Hydroformylation (oxo synthesis, Roelen reaction), in: B. Cornils, W.A. Herrmann (Eds.), Applied Homogeneous Catalysis with Organometallic Compounds, Vol. 1, VCH, New York, 1996.
[3] D. Evans, G. Yagupsky, G. Wilkinson, J. Chem. Soc. (A) (1968) 2660.
[4] D. Evans, J.A. Osborn, G. Wilkinson, J. Chem. Soc. (A) (1968) 3133.
[5] G. Yagupsky, C.K. Brown, G. Wilkinson, J. Chem. Soc. (A) (1970) 1392.
[6] C.K. Brown, G Wilkinson, J. Chem. Soc. (A) (1970) 2753.
[7] R.F. Heck, D.S. Breslow, J. Am. Chem. Soc. 82 (1960) 4438.
[8] D.S. Breslow, R.F. Heck, Chem. Ind. (London) (1960) 467.
[9] R.F. Heck, D.S. Breslow, J. Am. Chem. Soc. 83 (1961) 4023.
[10] R.F. Heck, D.S. Breslow, J. Am. Chem. Soc. 84 (1962) 2499.
[11] D.E. Morris, H.B. Tinker, CHEMTECH (1972) 554.
[12] T. Ueda, Proc. 5th Int. Congr. Catal. 1 (1973) 431.
[13] R.B. King, A.D. King, M.Z. Iqbal, J. Am. Chem. Soc. 101 (1979) 4893.
[14] A.A. Oswald, J.S. Merola, E.J. Mozeleski, R.V. Kastrup, J.C. Reisch, ACS Symp. Ser. 171 (1981) 503.
[15] A.A. Oswald, D.E. Hendriksen, R.V. Kastrup, J.S. Merola, J.C. Reisch, Preprints Div. Petr. Chem., ACS Natl. Meeting, Las Vegas, NV, Spring 27(2) (1982) 292.
[16] R.V. Kastrup, J.S. Merola, A.A. Oswald, Adv. Chem. Ser. 196 (1982) 43.
[17] J.M. Brown, L.R. Canning, A.G. Kent, P.J. Sidebottom, J. Chem. Soc., Chem. Commun. (1982) 721.
[18] J.M. Brown, A.G. Kent, J. Chem. Soc., Chem. Commun. (1982) 723.
[19] R.B. King, K. Tanaka, J. Indian Chem. Soc. 59 (1982) 124.
[20] W.R. Moser, C.J. Papile, D.A. Brannon, R.A. Duwell, S.J. Weininger, J. Mol. Catal. 41 (1987) 271.
[21] J.M. Brown, A.G. Kent, J. Chem. Soc., Perkin Trans. II (1987) 1597.
[22] I.T. Horvath, R.V. Kastrup, A.A. Oswald, E.J. Mozeleski, Catal. Lett. 2 (1989) 85.
[23] M. Garland, G. Bor, Inorg. Chem. 28 (1989) 410.
[24] D.T. Brown, T. Eguchi, B.T. Heaton, J.A. Iggo, R. Whyman, J. Chem. Soc., Dalton Trans. (1991) 677.
[25] G.A. Korneyeva, T.V. Vladimirova, M.M. Potarin, E.I. Khromushina, Ye.V. Slivinskii, S.M. Loktev, Petr. Chem. 33 (5) (1993) 391.
[26] P.C. d'Oro, L. Raimondi, G. Pagani, G. Montrasi, G. Gregorio, A. Andreetta, Chim. Ind. (Milan) 62 (1982) 572.
[27] B.M. Bhanage, S.S. Divekar, R.M. Deshpande, R.V. Chaudhari, J. Mol. Catal. A: Chem. 115 (1997) 247.
[28] R.M. Deshpande, Purwanto, H. Delmas, R.V. Chaudhari, Ind. Eng. Chem. Res. 35 (1996) 3927.
[29] S.S. Divekar, R.M. Deshpande, R.V. Chaudhari, Catal. Lett. 21 (1993) 191.
[30] R.M. Deshpande, R.V. Chaudhari, J. Catal. 115 (1989) 326.
[31] R.M. Deshpande, R.V. Chaudhari, Ind. Eng. Chem. Res. 27 (1988) 1996.
[32] V.I. Kurkin, V.V. Sakulin, A.K. Kobyakov, Ye.V. Slivinskii, Me.Y. Basner, R.A. Aronovich, G.A. Korneyeva, S.M. Loktev, Petr. Chem. 34 (5) (1994) 393.
[33] R.M. Deshpande, B.M. Bhanage, S.S. Divekar, R.V. Chaudhari, J. Mol. Catal. 78 (1993) L37.
[34] J.B. Claridge, R.E. Douthwaite, M.L.H. Green, R.M. Lago, S.C. Tsang, A.P.E. York, J. Mol. Catal. 89 (1994) 113.
[35] R.M. Deshpande, S.S. Divekar, R.V. Gholap, R.V. Chaudhari, Ind. Eng. Chem. Res. 30 (1991) 1389.
[36] J.D. Unruh, J.R. Christenson, J. Mol. Catal. 14 (1982) 19.
[37] M. Matsumoto, M. Tamura, J. Mol. Catal. 16 (1982) 209.
[38] O.R. Hughes, J.D. Unruh, J. Mol. Catal. 12 (1981) 71.
[39] J. Hjortkjaer, J. Mol. Catal. 5 (1979) 377.
[40] A.R. Sanger, J. Mol. Catal. 3 (1978) 221.
[41] W. Strohmeier, A. Kühn, J. Organomet. Chem. 110 (1976) 265.
[42] J.H. Craddock, A. Hershman, F.E. Paulik, J.F. Roth, I&EC Prod. Res. Dev. 8 (1969) 291.
[43] C.K. Brown, G. Wilkinson, Tetrahedron Lett. (1969) 1725.
[44] S.A. Miller, Al. Ekstrom, N.R. Foster, J. Chem. Eng. Data 35 (1990) 125.
[45] A. Bhattacharya, R.V. Chaudhari, Ind. Eng. Chem. Res. 26 (1987) 1168.
[46] R.L. Pruett, J.A. Smith, J. Org. Chem. 34 (1969) 327.
[47] K.L. Olivier, F.B. Booth, Hydrocarbon Processing (1970) 112.
[48] A. Hershman, K.K. Robinson, J.H. Craddock, J.F. Roth, I&EC Prod. Res. Dev. 8 (1969) 372.